Early Mars serpentinization-derived CH4 reservoirs, H-2-induced warming and paleopressure evolution

Eric Chassefière, Jérémie Lasue, Benoit Langlais, Yoann Quesnel

Early Mars serpentinization-derived CH_4 reservoirs, H_2 induced warming and paleopressure evolution

E. CHASSEFIÈRE[1], J. LASUE[2,3], B. LANGLAIS[4], Y. QUESNEL[5]

[1]GEOPS, Univ. Paris-Sud, CNRS, Université Paris-Saclay, Rue du Belvédère, Bât. 504-509, 91405 Orsay, France

[2]Université de Toulouse; UPS-OMP; IRAP; Toulouse, France

[3]CNRS; IRAP; 9 Av. colonel Roche, BP 44346, F-31028 Toulouse cedex 4, France

[4]LPG-CNRS, Université de Nantes, Nantes, France,

[5]Aix-Marseille Université, CNRS, IRD, CEREGE UM34, Aix-en-Provence, France

Submitted to Meteoritics & Planetary Sciences

Revised August 31, 2016

Abstract: CH_4 has been observed on Mars both by remote sensing and in situ during the past 15 years. It could have been produced by early Mars serpentinization processes that could also explain the observed Martian remanent magnetic field. Assuming a cold early Mars, a cryosphere could trap such CH_4 as clathrates in stable form at depth. The maximum storage capacity of such a clathrate cryosphere has been recently estimated to be $2\ 10^{19}$ to $2\ 10^{20}$ moles of methane. We estimate how large amounts of serpentinization-derived CH_4 stored in the cryosphere have been released to the atmosphere at the end of the Noachian and the beginning of the Hesperian. Due to rapid clathrate dissociation and photochemical conversion of CH_4 to H_2, these episodes of massive CH_4 release may have resulted in transient H_2-rich atmospheres, at typical levels of 10-20% in a background 1-2 bar CO_2 atmosphere. The collision-induced heating effect of H_2 present in such an atmosphere has been shown to raise the surface temperature above the water freezing point. Our results show that the early Mars cryosphere had a sufficient CH_4 storage capacity to have maintained H_2-rich transient atmospheres during a total time period up to several Myr or tens Myr, having potentially contributed to the formation of valley networks during the late Noachian and early Hesperian. Local and rapid destabilization of the cryosphere

by large events (such as the Hellas Basin or Tharsis bulge formation) may be at the origin of such release.

1. INTRODUCTION

The detection of methane on Mars by remote sensing from orbit and from the ground, as well as by in situ measurements from Mars surface, is now a well-established fact. During the year 2003 the measured CH_4 level reached up to 10 ppbv globally with local abundances up to 30 ppbv (Formisano et al., 2004; Mumma et al., 2009). Such high values were not replicated by later studies and an upper limit of 8 ppbv was derived from telescopic observations between 2006 and 2010 (Villanueva et al., 2013), while a local low upper limit of 1.3 ppbv was obtained during the first period of in situ observations performed by the Mars Science Laboratory (MSL) Curiosity rover at Gale Crater during the year 2012 (Webster et al., 2013). More recently, Curiosity detected significant amounts of CH_4 on its way to Mount Sharp. While the background level of CH_4 remains at the limit of detection of the rover (below 1 ppbv), an elevated level of CH_4 of 7.2 +/- 2.1 ppbv (i.e., the same level as previous remote sensing detections) was detected during four measurement sequences spanning approximately 2 months (Webster et al., 2015). However, observations by MSL over a second Mars year did not reveal any seasonal variation in the CH_4 level, which remained low since the first strong detection (G. Webster, D. Brown and L. Cantillo, 2016, Second Cycle of Martian Seasons Completing for Curiosity Rover, Press Release, May 11, 2016, http://mars.nasa.gov/msl/news). Detection of CH_4 by MSL, as well as by all existing remote sensing measurements of various spaceborne and terrestrial observatories, has been contested by K. Zahnle and D. Catling (Zahnle et al., 2011; Zahnle and Catling, 2015) which pointed out possible measurement artifacts : competing telluric absorption for ground-based measurements making them difficult to quantitatively interpret, low signal to noise ratio for orbit measurements, contamination by terrestrial methane for MSL in situ measurements. Although it cannot be definitely proven at present, the presence of CH_4 on Mars seems however highly likely, and its consequences deserve to be studied.

The presence of methane on Mars is an especially important topic as methane may have a biogenic origin (Atreya et al. 2006). There are other possible abiotic sources or processes to produce methane, and one of them is serpentinization (Oze and Sharma, 2005). This is a low-

pressure, low-to-medium temperature metamorphic process by which low-silica mafic rocks are hydrothermally altered, producing serpentine and magnetite, storing water and releasing dihydrogen. While this process may still be occurring today at depth, it could have been more common on early Mars when conditions included stronger volcanic activity, higher rates of large impact cratering and liquid water temporarily flowing on the surface (Solomon et al., 2005; Mangold et al., 2012; McSween et al., 2014). A large fraction of this water could have been easily trapped by serpentinization during the Noachian in hydrated, altered minerals at depth, while a significant amount of CH_4 may have been released in the atmosphere after Fisher-Tropsch reactions of H_2 within hydrothermal fluids converting CO_2 and H_2 into CH_4 (Chassefière et al., 2013a), and/or alternative processes (Etiope and Sherwood Lollar, 2013). In the presence of a global magnetic field, serpentinization may also explain the strong remanent magnetic field observed above the old southern terrains (Quesnel et al., 2009). Another interesting argument in favor of the early occurrence of this process on Mars is that the H_2 release and associated isotopic fractionation is consistent with the observed high D/H ratio in the present-day Martian atmosphere (Chassefière and Leblanc, 2011b).

Quantifying this phenomenon is rather difficult, but one can use magnetization models (Langlais et al., 2004; Morschhauser et al., 2014) to estimate the thickness of the magnetized, serpentinized layer, and so the amount of water trapped in hydrated minerals (Chassefière et al., 2013) as well as the CH_4 possibly-released during the crustal alteration. Under the assumption of a cold early Mars environment, a cryosphere could trap methane as clathrates in stable form at depth (Max and Clifford 2001; Chastain and Chevrier 2007). The extent and spatial distribution of these methane reservoirs were recently computed with respect to the magnetization distribution and other factors (Lasue et al., 2015). The maximum storage capacity of such a clathrate cryosphere is estimated to be 2.1×10^{19} - 2.2×10^{20} moles of CH_4. This quantity is based on the units which are still magnetized today, and can thus be seen as a minimum estimate, as it does not take into account the spatial extent of the structures that lost their magnetization at some time after their formation. This amount of trapped methane is sufficient for releases to have happened sporadically during the history of the planet at the level that has been detected remotely ($\sim1.2\times10^{9}$ moles). Such release events could have been more frequent and intense on early Mars at the time when valley networks formed.

Recent greenhouse calculations suggest that, unlike on Earth, CH_4 may not be an efficient greenhouse gas on Mars and may not have played a significant role in raising the surface temperature above the water freezing point (Ramirez et al., 2014). The collision-induced absorption caused by H_2 could have been much more efficient provided that the volume mixing ratio of H_2 in the atmosphere when valley networks formed was above ~5% (Ramirez et al., 2014). These authors used a one-dimensional radiative convective model to show that an atmosphere containing 4 bar of CO_2, with 5 % H_2, or 1.3 bar of CO_2, with 20% H_2, could have raised the mean surface temperature of early Mars above the freezing point of water. They proposed that H_2 could have been released from the reduced early Martian mantle through volcanic activity. Assuming that the input flux of H_2 had to be balanced by thermal escape of atomic hydrogen to space, they concluded that a continuous release of H_2 from the solid planet was required to maintain H_2 at a given level in the atmosphere, e.g. at least 4 10^{11} cm^{-2} s^{-1}, corresponding to an atmospheric H_2 mixing ratio of 2.5 % by using a simple 1D parametrized approach, and up to 10% for more complex simulations (Ramirez et al., 2014). The residence time of H_2 in the atmosphere with respect to escape is of the order of a few tens to a few hundred thousand years in the relevant ranges of CO_2 pressure and H_2 mixing ratio.

The main idea of the current study is to evaluate the possibility of a different source for the H_2 in the early Martian atmosphere, without excluding that a part of the released H_2 was related to volcanic activity. This alternative source could be associated with the photochemical decomposition of CH_4 previously stored in the cryosphere in the form of clathrates and later released. The direct trapping (together with CH_4) and subsequent release of H_2 in binary clathrates (Lunine and Stevenson, 1985) is not considered due to the lack of knowledge of H_2 clathrate thermodynamics. In the following we first review the sustainability of H_2 in the Martian atmosphere and existing constraints on the evolution of the atmospheric pressure on early Mars (section 2). In section 3, we briefly present existing models of the ancient Martian cryosphere, provide a quantitative estimate of H_2 input fluxes to the atmosphere, and model how several mechanisms were able to destabilize large amounts of clathrates at a global scale. Section 4 is devoted to a discussion of our results in view of existing estimates of the timescales of valley

network formation, in order to assess the ability of the proposed mechanism to maintain surface temperature above 0°C during a sufficient lapse of time.

2. CURRENT AND PAST INVENTORY OF H_2 IN THE MARTIAN ATMOSPHERE AND PALEOPRESSURE EVOLUTION

a. Sustainability of H_2 in the Martian atmosphere

The release to the atmosphere of CH_4 stored in the cryosphere in the form of clathrates results in an enhancement of the H_2 content of the atmosphere through the net reaction:

$$CH_4 + 2\ H_2O \rightarrow CO_2 + 4\ H_2 \qquad (1)$$

This conversion takes place under the action of solar UV photons breaking CH_4 into CH_x radicals which further react with OH radicals produced by photolysis of water. On present Mars, the photochemical lifetime of CH_4 is ~300 yrs (e.g., Lefèvre and Forget 2009). To explain sharp temporal and spatial variations of CH_4, as observed by remote sensing and in-situ observations, a much shorter lifetime is required, a few hundred days, at most, which necessarily involves heterogeneous reactions at the surface (Lefèvre and Forget 2009).

On present Mars, the thermal escape flux of hydrogen is not precisely known. Several estimates were made from remote sensing measurements onboard Mariner 6/7 (Anderson and Hord, 1971), Rosetta during its fly-by at Mars (Feldmann et al., 2011) and Mars-Express (Chaffin et al., 2014). They all suggest an average H escape flux in the range from 10^8 cm^{-2} s^{-1} to a few 10^8 cm^{-2} s^{-1}. According to both Mars Express observations (Chaffin et al., 2014) and a recently developed 3D atmosphere-exosphere coupling model (Chaufray et al., 2015), the H escape flux is however highly variable with season and solar cycle, from 10^7 cm^{-2} s^{-1} to more than 10^9 cm^{-2} s^{-1}. Recent MAVEN measurements made by the IUVS instrument (McClintock et al., 2014) have provided vertical H Ly-α scans from the surface up to 4000 km altitude, but no reliable estimate of the H escape flux can be done at this stage because more work is needed on calibration aspects (F. Leblanc, personal communication). The mixing ratio of H_2 in the atmosphere of Mars, derived

from UV measurements made at ~140 km altitude and extrapolated down to the surface by using photochemical models, is currently ~1.5 10^{-5} (e.g., Krasnopolsky and Feldmann, 2000). Assuming a typical average H escape rate of 10^8 cm^{-2} s^{-1}, the residence time of hydrogen atoms in the atmosphere with respect to escape is presently of the order of 2000 yrs.

Whether the lifetime of CH_4 is in the range from a few hundred years according to standard photochemical models to a few hundred days required to explain the observed methane plumes (Lefèvre and Forget 2009), it is definitely shorter than the residence time of H_2 molecules with respect to escape, by 1 or 2 orders of magnitude. It suggests that most hydrogen present in the atmosphere is in the form of H_2 and that the fraction of CH_4 not converted to H_2 in the atmosphere is small.

It is likely that a fraction of serpentinization-derived H_2 is released directly to the atmosphere, because all H_2 is not expected to be converted in CH_4 and therefore cannot be trapped in CH_4 clathrates. On Earth, hydrothermal vents release both CH_4 and H_2. As an example, the average H_2/CH_4 ratio in vents from deep sea hydrothermal systems is ~8 (Welhan and Craig, 1979). This ratio is quite variable from one place to the other, generally higher in continental hydrothermal systems (see references in Chassefière and Leblanc, 2011a), and unknown in the environmental conditions prevailing on ancient Mars. A fraction of the H_2 produced by serpentinization on Mars and not converted to CH_4 could be trapped in hypothesized H_2 clathrates, with a long retention time in the cryosphere, but the thermodynamics of H_2 clathrates is poorly known and no quantitative assessment of the H_2 clathrate storage capacity of the cryosphere can be done. Plausibly, the fate of most serpentinization-derived H_2 molecules not converted to CH_4 is to be rapidly released to the atmosphere because H_2 is a weakly chemically reactive molecule.

The potential role of outgassed serpentinization-derived H_2 in heating the surface of ancient Mars has been assessed by Batalha et al. (2015), but has been considered as probably minor with respect to the role of volcanic H_2. Besides, it is unlikely that episodes of high atmospheric H_2 may have persisted in this way, due to the long serpentinization time period (several 10^8 years) compared to the 7 10^4 yr residence time of hydrogen (as estimated in Section 4 for the atmosphere considered by Ramirez et al., 2014) with respect to thermal escape. Note that this

value of the residence time is more than one order of magnitude larger than the present value because of the different structures and chemical compositions of the ancient and present atmospheres. The trapping of serpentinization-derived H_2 in CH_4 clathrates offers an interesting possibility of long-term hydrogen storage, and subsequent sporadic discharges of hydrogen to the atmosphere when these clathrates dissociate. According to the net reaction (1), the storage capacity of 2.1×10^{19} - 2.2×10^{20} moles of CH_4 estimated by Lasue et al. (2015) corresponds to a total amount of available H_2 of 8.4×10^{19} – 8.8×10^{20} moles. For simplification purposes these values are rounded to ~ 10^{20} – 10^{21} moles. In the next section, we examine the plausibility of a 1.3-4 bar CO_2 atmosphere at 3.45-3.8 Ga.

b. Paleopressure of the Martian atmosphere

The initial CO_2 inventory of Mars is of the order of 100 bar or more (Lammer et al., 2013, and references therein), similar to Earth and Venus inventories. Most of the initial CO_2 has been lost to space by hydrodynamic escape at the very beginning, with a typical loss of 1 bar of CO_2 over typical time scales of 1-10 Myr (Tian et al., 2009). Hydrodynamic escape sharply decreased at ~4 Ga and passed below the volcanic outgassing rate at typically 3.9-4 Ga. At that time, the net flux of CO_2 to the atmosphere became positive, and an increase in pressure to a few 100 mbar between 4 Ga and 3.5 Ga cannot be excluded. It is generally thought that ~1 bar CO_2 may have been outgassed by volcanic activity during the first billion years of Mars history, and possibly until ~3 Ga, according to a temporal sequence which is poorly constrained (e.g. Werner, 2009; Grott et al., 2011; Baratoux et al., 2013). If indeed most of the volcanic activity and associated outgassing took place while the hydrodynamic escape was efficient, then only a small part of CO_2 (that outgassed after 4 Ga) would not have escaped, leaving only ~10%, or ~0.1 bar, of CO_2. On the contrary if the significant outgassing period extended later (until 3.5 or 3 Ga), more volcanic CO_2 may have remained on the planet (0.5 bar or more). The level and evolution of the CO_2 pressure postdating hydrodynamic escape on early Mars are not well known, but there are a number of observational constraints and modelling results consistent with a specific range of atmospheric pressure that we review (see below and in Table 1) in order to provide one possible paleopressure evolution scenario.

Observational constraints

The study of the size distribution of the impact craters can bring important constraints on the paleopressure. The atmosphere indeed acts as a filter and prevents the smallest objects from reaching the surface at high velocities to form craters (Melosh, 1989). The minimum size of observable craters therefore provides constraints on atmospheric density at the time when craters formed, or more precisely on its upper limit (Holsapple, 1993; Popova et al., 2003). Kite et al. (2014) analyzed craters in the Aeolis Dorsa region near Gale crater which contains a high density of preserved ancient craters interbedded with river deposits. They used high-resolution images and digital terrain models from the Mars Reconnaissance Orbiter to identify and characterize ancient craters dating back to about 3.6 Ga. They also used theoretical tools to predict what would be the actual crater size distribution for several levels of atmospheric pressures. By comparing these observed and theoretical distributions they concluded that the paleopressure was at most ~1 bar, possibly rising up to ~2 bar if rimmed circular mesas, interpreted to be erosionally-resistant fills or floors of impact craters, are excluded.

There are other constraints provided by different observations. Manga et al. (2012) analyzed a bomb sag in the Home Plate region, and concluded that the velocity of the impactor was 40 m s^{-1}. This implies a past atmospheric density which was at least 20 times larger than the current one, corresponding to a paleopressure larger than ~150 mbar. The outgassing history of Mars, as inferred from the $^{40}Ar/^{36}Ar$ ratio, predicts that a total of 1 bar of CO_2 was released in the atmosphere (Grott et al., 2011). The presence of Mg/Ca/Fe carbonates also suggests that the pressure was < 1 bar when they formed (Van Berk et al., 2012). Prehnite is a secondary Ca-Al phyllosilicate mineral usually formed by hydrothermalism in veins and cavities of basic rocks. It has been observed at a number of places on Mars (Ehlmann et al., 2011). It is unstable for CO_2 mole fraction in water larger than $2\ 10^{-3}$ (Ehlmann et al., 2011), implying a CO_2 atmospheric pressure not in excess of ~1 bar if water at depth was in equilibrium with the atmosphere (Kite et al., 2014). Another constraint is derived from the $^{40}Ar/^{36}Ar$ ratio in the atmospheric gas trapped in the 4.1 Gyr old ALH84001 meteorite, which may be used to constrain atmospheric pressure through an atmospheric ^{40}Ar evolution model (Cassata et al., 2012). The atmospheric evolution model used to interpret these data takes into account impact erosion, crustal outgassing and

meteorite accretion. Models fitting at best the ALH84001 Ar isotopic ratio suggest that pressure was smaller than 400 mbar at the late Noachian. All these constraints taken together suggest that paleopressure (when valley networks formed) ranged between ~150 mbar (from bomb sag) and 2 bar (from size distribution of ancient craters).

Model-consistent predictions

Chassefière et al. (2013b) studied the formation of CO_2-SO_2 clathrates on early Mars. As shown by these authors, if the atmospheric CO_2 pressure exceeds ~2 bar, the CO_2 in excess is trapped in CO_2 clathrates below the surface. Indeed, due to the increasing albedo of the atmosphere through Rayleigh scattering for increasing CO_2 pressure above 1 bar, the surface temperature induced by a p>~2 bar CO_2 atmosphere is smaller than the equilibrium temperature of clathrates, resulting in a saturation of CO_2 and its condensation in clathrates. Such a clathrate buffer would have maintained the CO_2 pressure close to ~2 bar, and the surface temperature close to 230 K, resulting in a cold Mars during the Noachian (Chassefière et al., 2013b). This result was obtained by using a one-dimension chemical radiative model of the atmosphere (Tian et al., 2010). Qualitative arguments show that using a 2-dimension, altitude-latitude, model, this upper limit of 2 bar may be somewhat lowered, but not below ~0.5 bar.

In the same paper, Chassefière et al. (2013b) showed that the early Mars cryosphere may have also trapped all the sulfur released by volcanism in the form of sulfur-rich CO_2-SO_2 clathrates, yielding the trapping of the equivalent of a pure SO_2 atmosphere of several tens to hundreds mbar. For a surface pressure lower than 2 bar and progressively decreasing, atmospheric sulfur is no longer trapped in clathrates, resulting in an increasing fraction of the atmospheric SO_2 which is released to the atmosphere and further convert to sulfate aerosols (Chassefière et al. 2013b; Schmidt et al., this issue). If the late sulfate deposition which occurred during the Hesperian is due to this mechanism, the resulting constraint is that pressure dropped below about 0.5 bar at the beginning of the Hesperian.

Efficient H_2 collision-induced heating requires a CO_2 atmospheric pressure of at least 1.3 bar in order to heat the surface of Mars above the freezing point of water (Ramirez et al., 2014).

Assuming that this mechanism played an efficient role, the consistency of their results with the pressure domains derived from both observational constraints and other modelling results can be checked.

All the observational constraints and model predictions previously described are summarized in Table 1 and in Figure 1.

Table 1 : Observational constraints and model-consistent predictions constraints on paleopressure of the early Martian atmosphere.

Observation or model-consistent prediction Principle of pressure estimate	Epoch	Pressure	Comments	Reference
Observational constraints				
Aeolis Dorsa Crater size distribution	Late Noachian/ Hesperian	< 2 bar	< 1 bar including circular mesas in the statistical analysis	Kite et al. 2014
Bomb sag at Home Plate	Uncertain (Noachian Amazonian)	> 120 mbar		Manga et al. 2012
$^{40}Ar/^{36}Ar$ in ALH 84001	Early Noachian	< 1.5 bar before 4.2 Ga < 400 mbar at 4.16 Ga	Use of an atmospheric evolution model to interpret data	Cassata et al. 2012
Geochemical modeling of Mg-rich carbonates formation at Comanche rock	Late Noachian	< 1 bar		Van Berk et al. 2012
Prehnite stability	Noachian	< 1 bar		Kite et al. 2014 Ehlmann et al., 2011
Modelling results				
Formation of sulfate deposits explained by CO_2-SO_2 clathrate decomposition(5)	Hesperian	Drop from <2 bar to below ~0.5 bar	Upper limit of 2 bar down to 0.5 bar using 2-dimensional model	Chassefière et al. 2013b
Saturation of CO_2 wrt clathrate formation(5)	Noachian	< 2 bar	Upper limit of 2 bar down to 0.5 bar using 2-dimensional model	Chassefière et al. 2013b
Heating above H_2O freezing point by CO_2-H_2 atmosphere	Hesperian	> 1.3 bar	Not strictly consistent with upper limits of 1 bar derived from some other constraints, but not in strong disagreements due to large uncertainties.	Ramirez et al. 2014
Loss of initial CO_2 (~100 bar or more) by hydrodynamic escape	Early Noachian	100 bar loss in a few 100 Myr	Thermal escape stops at ~4 Ga	Tian et al. 2009
Volcanic outgassing	Mainly Noachian-early Hesperian	< ~1 bar		Grott et al. 2011

We propose in Figure 1 a possible temporal evolution of the paleopressure at the Noachian and the Hesperian consistent with most existing constraints or model- predictions. This simple scenario consists of an initially large pressure with a subsequent continuous decrease of the pressure due to hydrodynamic escape during early Noachian followed by a stabilization of the pressure around 1.5 bar, compatible with most observational and modelling constraints. A drop of the pressure from 1.5 bar to below 0.5 bar occurs during the Hesperian, potentially explaining the formation of massive sulfate deposits in this epoch due to the decomposition of CO_2-SO_2 clathrates (Schmidt et al., this issue), and is compatible with the constraint derived from crater analysis. This evolution curve is only indicative. For example, as previously noted, an increase of the pressure by several 100 mbar after the end of hydrodynamic escape, at about 4 Ga, may have occurred through volcanic production of CO_2. Note that our evolution curve doesn't fit the constraint derived from the analysis of argon isotopes in ALH84001 combined with a model of early atmospheric evolution.

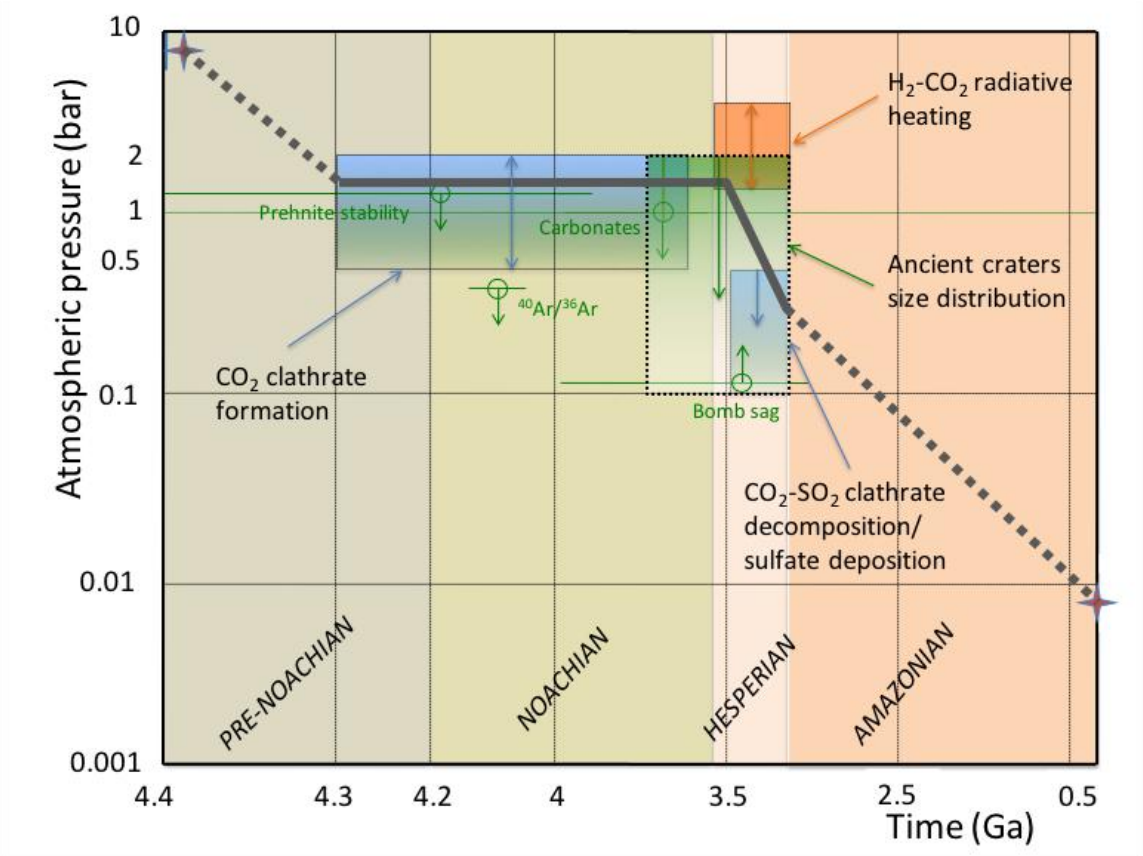

Figure 1: Existing observational, geochemical modelling and theoretical constraints on paleopressure of the Martian atmosphere (colored boxes and circles with arrows) and derived scenario of pressure evolution (thick black line). Observational and modelling constraints are represented by, respectively, green and black texts and box contours. The scenario consists in (i) an initially large pressure with a subsequent continuous decrease of the pressure due to hydrodynamic escape; (ii) then a stabilization of the pressure around 1.5 bar, compatible with both the upper limit of 2 bar, above which CO_2 condenses into clathrates at the Noachian (left blue box), and the lower limit of 1.3 bar, below which the addition of H_2 is not efficient in raising the surface temperature above the H_2O freezing point at the Hesperian (orange box); (iii) a drop of the pressure from 1.5 bar to below 0.5 bar, which could explain the formation of massive sulfate deposits at this epoch due to the decomposition of CO_2-SO_2 clathrates (right blue box), and is compatible with the constraint derived from crater analysis (green box). Adapted from Kite et al. (2014).

3. MODELS FOR THE RELEASE OF METHANE ON MARS

a. Models of Noachian cryosphere

Under cold early Mars conditions, a subsurface cryosphere covering the planet would form. The depths it would reach would depend on the surface equilibrium temperature of the planet, its geothermal heat flux Q_g, together with the material properties of the crust such as its thermal conductivity and porosity at depth. In this study, we use results from a univariate finite difference model of the cryosphere detailed in (Clifford et al., 2010; Lasue et al., 2013) for a clathrate saturated cryosphere.

The subsurface porosity decreases exponential based on a gravitational scaling of the lunar regolith porosity in the subsurface (exponential decreases with decay constant of 2.82 km starting at surface values of either $\Phi(0)=20\%$ or $\Phi(0)=35\%$, Clifford 1993). The noachian thermal heat flux was most probably larger than 50 $mW.m^{-2}$ (McGovern et al., 2002; Grott et al., 2007). Here, we assume two different heat fluxes for our estimation: one hot at 100 $mW.m^{-2}$ and another cold at 50 $mW.m^{-2}$.

From these values and with $\Phi(0)=20\%$, we can calculate the average depth of a clathrate cryosphere boundary at 273K as shown in Figure 2. The depth ranges from 800m below the equator to about 2.5km under the pole for $Q_g = 100 mWm^{-2}$ and it practically doubles to 2km and 5.5km for $Q_g = 50 mWm^{-2}$. This provides a lower limit on the quantity of trapped water for each case as clathrates can be stable at somehow higher temperatures if the pressure is high. The cryosphere trapped water ranges from 250m GEL for $Q_g = 100 mWm^{-2}$ to 400m GEL for $Q_g = 50 mWm^{-2}$. Higher values of 400m GEL and 660m GEL are obtained in the case where $\Phi(0)=35\%$.

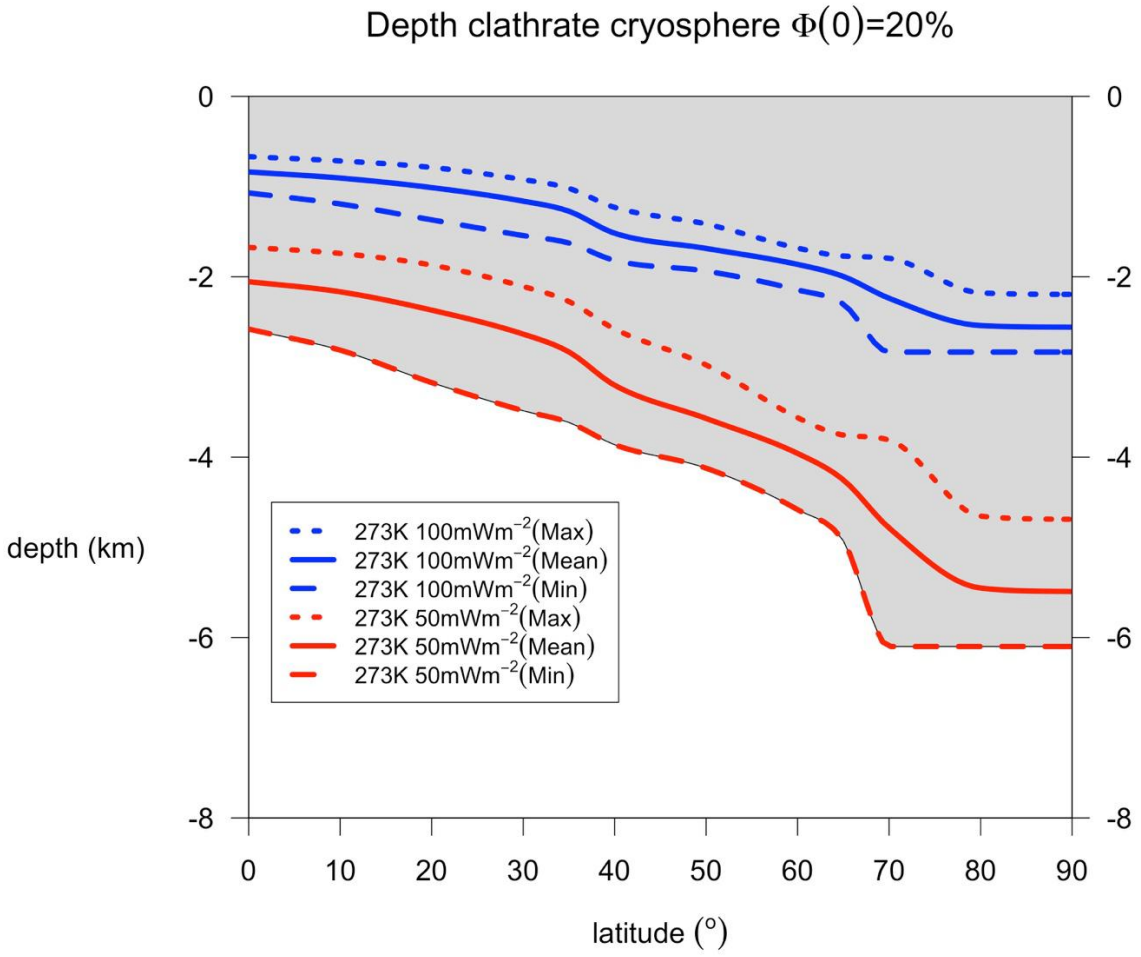

Figure 2 : Depth of a clathrate cryosphere as a function of the latitude with an exponential decay of porosity starting at 20% on the surface, and for 50 and 100 $mW.m^{-2}$ geothermal heat fluxes. (adapted

from the Clifford et al., 2010 subsurface model). The maximum and minimum variations due to the obliquity and eccentricity variations of Mars orbit are shown (based on Laskar 2004 simulations).

b. Serpentinization-derived methane trapped in early cryosphere as a possible source of warming-inducing H_2

We now consider the potential release to the atmosphere of CH_4 molecules produced by early serpentinization and stored as clathrates in the cryosphere. These molecules are then converted into H_2 molecules in the atmosphere by photochemical processes and may have a role in warming the early atmosphere. From the CH_4 storage capacity calculated by Lasue et al. (2015), we have derived a H_2 storage capacity of ~ 10^{20} – 10^{21} moles. According to the model of paleopressure evolution previously proposed, we will assume a typical CO_2 pressure of 1.5 bar, possibly varying in the range from 1.3-2 bar, at the time when valley networks formed. In this range, a 80% CO_2-20% H_2 atmosphere can heat the surface up to 273-285 K, and a 90% CO_2-10% H_2 atmosphere can heat the surface up to 250-270 K (Ramirez et al., 2014). Because these values are calculated using a one-dimensional climate model, even if the globally averaged temperature is slightly smaller than 273 K, the surface temperature is expected to locally raise above the water freezing point at a number of places and seasons during one Martian year.

In a steady state, the input flux of H_2 is balanced by thermal escape of atomic hydrogen to space. Indeed, because the thermal escape flux of hydrogen is proportional to the mixing ratio of H_2 in the atmosphere, the steady state value of the hydrogen escape flux is controlled by the value of the H_2 input flux. In models, a continuous release of H_2 from the solid planet must be included to maintain H_2 at a given level in the atmosphere, e.g. 4 10^{11} cm^{-2} s^{-1} for an atmospheric H_2 mixing ratio of 2.5 % (Ramirez et al., 2014). In order to maintain a H_2 mixing ratio in the range from 10% to 20% (4 to 8 times 2.5%), the input flux must be in the range from 1.6 - 3.2 10^{12} cm^{-2} s^{-1} (4 to 8 times 4 10^{11} cm^{-2} s^{-1}). This range converts into 1-2 10^6 moles s^{-1} when converting molecules in moles and integrating column densities over the whole Martian surface. Assuming a H_2 storage capacity of 10^{21} moles, and a H_2 input flux of 10^6 moles s^{-1}, such a flux can be maintained during ~30 Myr. For a storage capacity of 10^{20} moles, and a H_2 input flux of 2 10^6 moles s^{-1}, this time is ~1.5 Myr. The reservoir formed by serpentinization-derived CH_4 stored in the early cryosphere is therefore able to feed up the atmosphere with H_2 at the required level of

10-20% during a total duration ranging between ~1.5 and ~30 Myr, contributing to create conditions favorable to the presence of liquid water at the surface.

The residence time of H_2 in the atmosphere may be calculated by dividing the H_2 content of the atmosphere by the value of the escape rate. Assuming a 1.5 bar CO_2 atmosphere, and a 10% H_2 volume mixing ratio, the column density of H_2 is ~4 10^{24} cm^{-2}, which corresponds to a total content of 2.5 10^{18} moles. Assuming a H escape rate of ~[1.6 10^{12}]/2 cm^{-2} s^{-1} (case of an atmospheric H_2 mixing ratio of 10%, Ramirez et al., 2014), the lifetime of H_2 versus escape is ~7 10^4 yr = 0.07 Myr. If the storage capacity of H_2 is 10^{20} moles, the quantity of H_2 trapped in clathrates is equivalent to 40 times the amount of H_2 required to fill the atmosphere at the 10% H_2 mixing ratio level. The maximum number of individual outgassing events able to heat the surface above H_2O freezing temperature is 40. The duration of such ideal single events is 0.07 Myr. Up to 40 outgassing events, each one of 0.07 Myr, with a total or cumulated duration of 3 Myr, may occur. For a H_2 storage capacity of 10^{21} moles, the maximum number of events is 400, with a total duration of 30 Myr. For a H_2 storage capacity of 10^{20} moles, and a 20% H_2 mixing ratio level, the maximum number of events is 20, with a total duration of 1.5 Myr. At the other extreme, the release episode may consist of one single continuous big event during ~1.5 to ~30 Myr. All intermediate cases, from a low number of big events to a large number of small events, are possible. This total duration of 1.5-30 Myr is an upper limit, because the H_2 mixing ratio possibly can exceed the 10-20% range. But, on the other hand, the true amount of H_2 stored in the cryosphere may have been larger than our assumed range of 10^{20}-10^{21} moles, if large zones where serpentinization occurred have been later demagnetized.

Interestingly, an increase of the H_2 content of the atmosphere, followed by an increase of the surface temperature, is expected to further destabilize clathrates, with more and more H_2 in the atmosphere. Due to this positive feedback, a warm event could be more intense and last longer, although the total duration of warm events is limited by the amount of available CH_4 in the subsurface reservoir, and cannot be larger than a few million or tens million years.

The time scales for formation of the ancient Martian valley networks have been estimated by Hoke et al. (2011). They studied and modelled seven of the largest ancient valley networks on

Mars. With runoff rates similar to intense storms in arid regions on Earth, they found that the minimum formation time scales of these Martian valley networks are in the range from 0.1 to 10 Myr, depending on the specific valley network. These times are similar to the time scales previously estimated for the release of serpentinization-derived H_2 at a sufficient level to maintain a H_2 mixing ratio of 10-20% in a background CO_2 atmosphere of ~1.5 bar. They fit existing observations and models of valley formation much better than the hypothesis that warm episodes are primarily caused by impact events (e.g., Segura et al., 2008). This last hypothesis would require strong hurricane-scale flows able to form large valley network formations in as little as a few thousand years, which is not the favored interpretation (Hoke et al., 2008).

c. Cryosphere destabilization

The origin of sporadic and massive destabilization of CH_4 clathrates at the end of the Noachian and during the Hesperian is not straightforward. One possible cause is the rapid decrease of the CO_2 pressure starting at the end of the Noachian (Fig. 1), which inhibited the formation of clathrates at the surface and favored their decomposition, as it could have occurred for SO_2-rich clathrates formed from sulfur released by volcanic eruptions (Schmidt et al., this issue). For CH_4 clathrates, formed at depth by serpentinization processes, a pressure drop can explain their dissociation only if they are in contact with the atmosphere, which requires a quite porous and/or fractured upper crust. Generally speaking, large impacts may have played a role in destabilizing clathrates, but there is no reason for an increase of impact rates at the end of the Noachian and beginning of the Hesperian.

Here we study the consequences of three destabilization events. Two are destructive and very localized (impact and volcano), while the third has a larger extent and is related to true polar wander, possibly as a consequence of the two first events. The rise of Tharsis is one of the best candidate to explain major destabilization events: not only would it locally increase the crustal thermal gradient (at least within and around its bulge), but it would also release large amounts of volcanic H_2O (so H_2), CO_2, CH_4 and SO_2 in the atmosphere (Gaillard and Scaillet, 2009), which enhanced the greenhouse effect (Phillips et al., 2001). By destabilizing clathrates, potentially huge amounts of gases stored in the crust, like CH_4 (this paper) and SO_2 (Schmidt el al., this

issue), could have been released to the atmosphere. Interestingly the growth of Tharsis bulge (around 3.7 Ga) resulted in a possible polar wander, thus modifying the illumination conditions at the equator. It was recently suggested (Bouley et al., 2016) that this took place after the valley networks formed, i.e., closer to 3.5 Gyr and later than it was previously thought (e.g., Zhong, 2009). The addition of all these consequences of the Tharsis rise may have destabilized the clathrates.

We approximately calculated the effect of each type of events on the Noachian cryosphere. We can estimate a minimum effect of the true polar wander of Mars by considering the destabilization of clathrates located at depth under a spherical segment around the equator, between 20 degrees latitude North and 20 degrees latitude South (20° being a lower limit based on the simulations by Bouley et al. 2016). Clathrates at higher latitudes will also be impacted, but the effects will be less due the smaller areas and a smaller amplitudes of the temperature changes involved. We simulated the effect of the Tharsis Bulge rise formation by integrating the cryosphere volume located at depth below a circle covering the surface of the Tharsis Bulge. We also estimate the consequences of a giant impact which could also have destabilized the cryosphere, and consider the case of the Hellas impact basin, which formed between 3.9 and 4.1 Ga (Robbins et al., 2013). For this purpose, the radius of the circle considered is twice that of the visible impact since models of the impact formation indicate that the ejected melting sheet thermally affects a surrounding area up to two radii away from the center of impact (Ivanov et al., 2010). For each scenario, we assume that the whole cryosphere (before impact or before the emplacement of Tharsis) is made of clathrates, so that the values obtained are upper limits to the quantity of methane that can be involved in the process, and because the events erased the remanent crustal magnetic field that was present at that time (if any), and which was used to estimate the trapped clathrates in Lasue et al. (2015). We also consider 2 different subsurface porosity variations based on a gravitational scaling of the lunar regolith porosity in the subsurface (exponential decreases with decay constant of 2.82 km starting at surface values of either $\Phi(0)=20\%$ or $\Phi(0)=35\%$, Clifford 1993) and assume two different heat fluxes for the Noachian era: one hot at 100 $mW.m^{-2}$ and another cold at 50 $mW.m^{-2}$. Table 2 summarizes the values obtained for each case. Previous calculations of the amount of water released in the

martian atmosphere by large impacts of sizes relevant to the case of Hellas are coherent with the values that we obtain (Segura et al., 2002).

Table 2: Trapping volume of local Noachian cryosphere under different destabilization scenarios
The results for TPW appear insensitive to the geothermal heat flux, due to the fact that the change of porosity at depth almost compensates the variation in volume destabilized due to surface temperature change.

		Hellas Planitia impact basin		*Tharsis Bulge formation*		*True Polar Wander destabilization of equator*	
	Q_g (mW m^{-2})	*100*	*50*	*100*	*50*	*100*	*50*
$\Phi(0) = 0.20$	GEL* (m)	9	13.6	6.7	11.7	9.7	10.0
	CH4 (m3)	2.1E+17	3.2E+17	1.6E+17	2.8E+17	2.3E+17	2.4E+17
	CH4 (mol)	9.5E+18	1.4E+19	7.1E+18	1.2E+19	1.0E+19	1.1E+19
	H2 (mol)	3.8E+19	5.7E+19	2.8E+19	4.9E+19	4.1E+19	4.2E+19
$\Phi(0) = 0.35$	GEL (m)	13.2	22	10.4	18.5	17.1	17.6
	CH4 (m3)	3.1E+17	5.2E+17	2.5E+17	4.4E+17	4.1E+17	4.2E+17
	CH4 (mol)	1.4E+19	2.3E+19	1.1E+19	2.0E+19	1.8E+19	1.9E+19
	H2 (mol)	5.6E+19	9.3E+19	4.4E+19	7.8E+19	7.2E+19	7.4E+19

*GEL : Global Equivalent Layer. A 1 m deep GEL corresponds to the volume of a uniform layer of 1 m depth covering the whole planet.

While sudden clathrate dissociation can be argued to have occurred on a small geologic time scale for the rise of the Tharsis bulge and the formation of Hellas impact basin, it is not the case for the destabilization of clathrates near the equator following the true polar wander. Indeed, the latter case will lead to a different surface equilibrium temperature, and a change in the depth of the cryosphere base, which is induced by the heat wave propagation at such depth (see also Tsai and Stevenson, 2007, for other theoretical problems with TPW speed). The depth that needs to be considered in the cases calculated here ranges from approximately 1 to 2.5km. A simple solution to the Fourier unidimensional heat transfer equation gives a timescale estimate, τ, based on :

$$\tau = \frac{d^2 \rho c_p}{k}$$

where d is the depth of the base of the cryosphere, ρ, the density of the material, c_p, the heat capacity of the material and k, the thermal conduction. Using approximate values that are relevant for basalt: 3000 $kg.m^{-3}$ for the density, 1000 $J.kg^{-1}.K^{-1}$ for the heat capacity, a range of 2.24 to 3.64 $W.m^{-1}.K^{-1}$ for the thermal conductivity (Clifford et al., 2010) and depths of 1 km to 2.5 km for the cryosphere, then the typical timescale for the heat wave to impact these depths is between 26000 years and 0.2 Myr. Theoretical considerations also limit strongly the speed of TPW effect. A typical speed of TPW is about 1 degree per million years (Tsai and Stevenson 2007; Chan et al., 2014). This speed would be so slow as to prevent any significant clathrates release in the span of time considered for the atmospheric changes to have occurred. Clathrates redistribution will likely happen at depth without much effect on the surface of the planet.

The three events we consider give similar results in terms of potentially released H_2. They could have destabilized methane and released between $3x10^{19}$ and $9x10^{19}$ moles of H_2 per event. As shown above this would be sufficient to alter the thermal state of the planet and generate a long-lived (0.1 to several Myr) global warm episode for Mars climate. However, the duration of the release associated with the polar wander was most likely too long, it is therefore unlikely to have played a major role in the global climate change due to the long timescales involved for both the true polar wander to happen and the heat wave conduction through the crust. Only Tharsis- or Hellas-like events could have played a significant role in sporadically releasing enough H_2 to lead to warm episodes.

4. DISCUSSION

It has been demonstrated that the CH_4 trapping capacity of the early Martian cryosphere is at least of the same order of magnitude than the quantity of CH_4 possibly released by early serpentinization processes that would have been necessary to generate the observed Martian remanent magnetic field (Quesnel et al., 2009; Lasue et al., 2015). The presence of such clathrate reservoirs could explain the sporadic release of CH_4 at the surface of the planet to this day. Much larger amount of CH_4 should have been released to the atmosphere during the much more active volcanic periods during the first billion years, as well as at the times when large impacts occurred. Due to rapid photochemical conversion of CH_4 into H_2 in the atmosphere, large CH_4

outbursts could have resulted in H_2 mixing ratios larger than 10% in the background 1-2 bar CO_2 atmosphere, allowing a significant collision-induced greenhouse heating raising surface temperature above, or close to, the water freezing point. The cumulated period of large H_2 level could have been as long as a few million to ten million years during Hesperian times, due to potentially large amounts of CH_4 stored in the early cryosphere due to serpentinization.

The time scales for formation of the ancient Martian valley networks have been estimated by Hoke et al. (2011). They studied and modelled seven of the largest ancient valley networks on Mars. With runoff rates similar to intense storms in arid regions on Earth, they found that the minimum formation time scales of these Martian valley networks are in the range from 0.1 to 10 Myr, depending on the specific valley network. These times are similar to the time scales previously estimated for the release of serpentinization-derived H_2 at a sufficient level to maintain a H_2 mixing ratio of 10-20% in a background CO_2 atmosphere of ~1-2 bar. They fit existing observations and models of valley formation better than the hypothesis that warm episodes are primarily caused by impact events (e.g., Segura et al., 2008). This last hypothesis would require strong hurricane-scale flows able to form large valley network formations in as little as a few thousand years, which is not the favored interpretation (Hoke et al., 2008).

Quantitative estimates made in this paper are orders of magnitude rather than precise values, due to large uncertainties on past serpentinization rates and the amount of methane stored in the cryosphere. This amount may have been smaller than estimated in the present paper for different reasons. First, the CH_4 storage capacity of the cryosphere has been calculated assuming that it was formed only of CH_4 clathrate, which is likely not the case, since other clathrates (CO_2, SO_2, …) and pure ice may be part of the cryosphere. Second, all the H_2 produced by serpentinization was likely not converted to CH_4, as observed on Earth, and the non-converted H_2 has potentially been released to the atmosphere at slow rate over long periods, with no accumulation in the cryosphere and further sudden release, not allowing a significant increase of the atmospheric H_2 mixing ratio. Additionally, if most CH_4 outgassing events have been too small to generate a 10-20% H_2 mixing ratio atmosphere, only a limited part of the stored hydrogen has been involved in planetary warming. If most events have been strong, yielding H_2

mixing ratios in the atmosphere much in excess of 10-20%, the total duration of the planetary warming could have been shorter.

On the other hand, the cumulated amount of CH_4 formed by serpentinization, estimated from the amount of rocks still magnetized today, may be underestimated if some serpentinization zones have been demagnetized postdating their formation, yielding a global underestimate of the mechanism proposed in this paper

Despite uncertainties, our scenario may potentially explain the occurrence of conditions favorable to the formation of valley networks. It requires that the atmospheric CO_2 pressure at the end of the Noachian was 1-2 bar. Better constraining the evolution of Mars atmospheric pressure since 4 Ga is a major challenge for understanding better Mars ancient climate.

5. CONCLUSION

We suggest that rapid CH_4 clathrate dissociation and photochemical conversion of CH_4 to H_2 occurred at the end of the Noachian and during the Hesperian. These episodes of massive CH_4 release may have resulted in transient H_2-rich atmospheres, at typical levels of 10-20% in a background 1-2 bar CO_2 atmosphere, raising the surface temperature above the water freezing point and allowing the formation of valley networks. The typical major geological events such as the rise of the Tharsis bulge or the Hellas impact basin formation could have destabilized CH_4 and injected in the atmosphere a quantity of H_2 between 3×10^{19} and 9×10^{19} moles per event. This would be sufficient to alter the thermal state of the planet and generate a long-lived (0.1 to several Myr) global warm episode for Mars climate. The true polar wander of the planet could also have destabilized a significant amount of clathrates at depth, but is unlikely to have played a major role in the global climate change due to the long timescales involved for the heat wave conduction through the crust.

ACKNOWLEDGEMENTS

We thank S. Clifford and two anonymous reviewers for improving the manuscript through thorough and constructive reviews. We acknowledge support from “Institut National des Sciences de l’Univers” (INSU) and « Groupe Système Solaire » of the "Centre National d’Etude Spatiale" (CNES) through the "Programme National de Planétologie", and the "Centre National de la Recherche Scientifique" (CNRS) through the EPOV interdisciplinary program. One of us (Y. Q.) thanks the OSU Institut Pytheas.

REFERENCES

Anderson Jr D.E., and Hord C.W. 2011. Mariner 6 and 7 ultraviolet spectrometer experiment: Analysis of hydrogen Lyman-alpha data. *J. Geophys. Res.* 76, 6666-6673.

Atreya S. K., Mahaffy R. P., Wong, A. 2006. Methane and related trace species on Mars: Origin, loss, implications for life, and habitability. *Planet. Space Sci.* 55, 358-369.

Baratoux D., Toplis M.J., Monnerea, M., and Sautter, V. 2013. The petrological expression of early Mars volcanism, *J. Geophys. Res. Planets* 118, Issue 1, 59-64.

Batalha N., Domagal-Goldman S.D., Ramirez R., and Kasting J. F .2015. Testing the early Mars H_2-CO_2 greenhouse hypothesis with a 1-D photochemical model. *Icarus* 258, 337-349.

Bouley S., Baratoux D., Matsuyama I., Forget F., Séjourné A., Turbet M., and Costard F. 2016. Late Tharsis formation and implications for early Mars, *Nature* 531, 344-347, DOI: 10.1038/nature17171.

Cassata W.S., Shuster D.L., Renne P.R., and Weiss B.P. 2012. Trapped argon isotopes in meteorite ALH 84001 indicate Mars did not have a thick ancient atmosphere. *Icarus* 221, 461-465. Doi: 10.1002/2013GL058578.

Chaffin M.S., Chaufray J.-Y., Stewart A.I., Montmessin F., Schneider, N.M., and Bertaux J.-L. 2014. Unexpected variability of of martian hydrogen escape. *Geophys. Res. Lett.* 41, 314-320.

Chan N. H., Mitrovica J. X., Daradich A., Creveling J. R., Matsuyama I., and Stanley S. 2014. Timedependent rotational stability of dynamic planets with elastic lithospheres. *J. Geophys. Res. Planets* 119(1), 169-188.

Chassefière E., and Leblanc F. 2011a. Explaining the redox imbalance between the H and O escape fluxes at Mars by the oxidation of methane. *Planet. Space Sci.* 59, 218-226.

Chassefière E., and Leblanc F. 2011b. Constraining methane release due to serpentinization by the observed D/H ratio on Mars. *Earth Planet. Sci. Let.* 310, 262–271, doi: 10.1016/j.epsl.2011.08.013.

Chassefière E., Langlais B., Quesnel Y., and Leblanc F. 2013a. The fate of early Mars' lost water: The role of serpentinization. *J. Geophys. Res.* 118, 1123–1134. doi: 10.1002/jgre.20089.

Chassefière E., Dartois E., Herri J.-M., Tian F., Schmidt F., Mousis O., and Lakhlifi A. 2013b. CO_2-SO_2 clathrate hydrate formation on early Mars. *Icarus* 223, 878-891.

Chastain B. K., and Chevrier, V. 2007. Methane clathrate hydrates as a potential source for martian atmospheric methane. *Planet.Space Sci.* 55(10), 1246-1256.

Chaufray J.-Y., Gonzalez-Galindo F., Forget F., Lopez-Valverde M.A., Leblanc F., Modolo R., and Hess S. 2015. Variability of the hydrogen in the martian upper atmosphere as simulated by a 3D atmosphere-exosphere coupling. *Icarus* 245, 282-294.

Clifford S.M., Lasue J., Heggy E., Boisson J., McGovern P., and Max M.D. 2010. Depth of the Martian cryosphere: Revised estimates and implications for the existence and detection of subpermafrost groundwater. *J. Geophys. Res.* 115, E07001. doi: 10.1029/2009JE003462.

Clifford S.M. 1993. A model for the hydrologic and climatic behaviour of water on Mars. *J. Geophys. Res.* 98, 10973–11016. doi: 10.1029/93JE00225.

Ehlmann B.L., Mustard, J.F., Clark R.N., Swayze G.A., and Murchie S.L. 2011. Evidence for low-grade metamorphism, hydrothermal alteration, and diagenesis on Mars from phyllosilicate mineral assemblages, *Clays and Clay Minerals*, 59(4):359. DOI: 10.1346/CCMN.2011.0590402.

Etiope G., and Sherwood Lollar, B. 2013. Abiotic methane on Earth, Rev. Geophys., 51, 276-299.

Farley K. A., Malespin C., Mahaffy P., Grotzinger J. P., Vasconcelos P. M., Milliken R. E., ... and Grant J. A. 2014. In situ radiometric and exposure age dating of the Martian surface. *Science* 343(6169), 1247166.

Feldmann P.D., et al. 2011. Rosetta-ALICE observations of exospheric hydrogen and oxygen on Mars. *Icarus* 214, 394-399.

Formisano V., Atreya S., Encrenaz T., Ignatiev N., and Giuranna M. 2004. Detection of Methane in the Atmosphere of Mars. *Science* 306:1758-1761. doi: 10.1126/science.1101732.

Gaillard F., and Scaillet B. 2009. The sulfur content of volcanic gases on Mars. *Earth Planet. Sci. Lett.* 279 (1-2), 34-43.

Grott M., Morschhauser A., Breuer D., and Hauber E. 2011. Volcanic outgassing of CO_2 and H_2O on Mars. *Earth Planet. Sci. Lett.* 308, 391-400.

Hoke M.R.T., Hynek B.M., and Tucker G.E. 2011. Formation time scales of large Martian valley networks. *Earth Planet. Sci. Lett.,* 312, 1-12.

Holsapple K. A. 1993. The scaling of impact processes in planetary sciences. *Ann. Rev. Earth Planet. Sci.* 21, 333–373, doi:10.1146/annurev.ea.21.050193.002001.

Ivanov B. A., Melosh H. J., and Pierazzo E. 2010. Basin-forming impacts: Reconnaissance modeling. *Geological Society of America Special Papers*, *465*, 29-49.

Kite E.S., Williams J.-P., Lucas A., and Aharonson O. 2014. Low paleopressure of the martian atmosphere estimated from the size distribution of ancient craters. *Nat. Geosci*., 7, 335-338, doi: 10.1038/ngeo2137.

Krasnopolsky V.A., and Feldmann P.D. 2001. Detection of molecular hydrogen in the atmosphere of Mars. Science 294, 5548, 1914-1917.

Lammer H., Chassefière E., Karatekin O., Morschhauser A., Niles P.B., Mousis O., Odert P., Möstl U.V., Breuer D., Dehant V., Grott M., Gröller H ., Hauber E., and San Pham L.B. 2013. Outgassing history and escape of the Martian atmosphere and water inventory. *Space Sci. Rev.* 174(1-4), 113-154.

Langlais B., and Quesnel Y. 2008. New perspectives on Mars'anglais, B. and Quesnel, *C. R. Geoscience*. 340:791-800. doi: 10.1016/j.crte.2008.08.006.

Langlais B., Purucker M.E., and Mandea M. 2004. Crustal magnetic field of Mars. *J. Geophys. Res.* 109:E2. doi: 10.1029/2003JE002048.

Lasue J., Mangold N., Hauber E., Clifford S., Feldman W., Gasnault O., Grima C., Maurice S., and Mousis O. 2013. Quantitative Assessments of the Martian Hydrosphere. *Space Sci. Rev.* 174:155-212.doi: 10.1007/s11214-012-9946-5.

Lasue J., Quesnel Y., Langlais B., and Chassefière E. 2015. Methane storage capacity of the early martian cryosphere. *Icarus*. 260, 205-214.

Lefèvre F., and Forget F. 2009. Observed variations of methane on Mars unexplained by known atmospheric chemistry and physics. *Nature* 460, 7256, 720-723.

Lunine J.I., and Stevenson D.J. 1985. Thermodynamics of clathrate hydrate at low and high pressures with applicatio to the outer solar system. *Astrophys. J. Suppl. Ser.* 58, 493–531 (1985)

Manga M., Patel A., Dufek J., and Kite E.S. 2012. Wet surface and dense atmosphere on early Mars suggested by the bomb sag at Home Plate, Mars. *J. Geophys. Res*. 39, L01202, doi: 101029/ 2011GL050192.

McClintock W.E., Schneider N.M., Holsclaw G.M., Clarke J.T., Hoskins A.C., Stewart I., Montmessin F., Yelle R.V., and Deighan J. 2014. The Imaging Ultraviolet Spectrograph (IUVS) for the MAVEN Mission, *Space Sci. Rev.*, DOI 10.1007/s11214-014-0098-7.

McSween Jr. H.Y., Labotka T.C., and Viviano-Beck C.E. 2014. Metamorphism in the Martian crust. *Meteorit. Planet. Sci.*, 1-14, doi:10.1111/maps.12330.

Max M.D., and Clifford S.M. 2001. Initiation of the Martian outflow channels: related to the dissociation of gas hydrate? *Geophys. Res. Lett.* 28,9,1787-1790.

Melosh H.J., 1989. Impact Cratering: A Geologic Process. Oxford University Press, New York.

Milbury C., Schubert G., Raymond C.A., Smrekar S.E., and Langlais B. 2012. The history of Mars' dynamo as revealed by modeling magnetic anomalies near Tyrrhenus Mons and Syrtis Major, *J. Geophys. Res.*, 117.

Mousis O., Chassefière E., Lasue J., Chevrier V., Elwood Madden M. E., Lakhlifi A., Lunine J.I., Montmessin F., Picaud S., Schmidt F., and Swindle T.D. 2013. Volatile Trapping in Martian Clathrates. *Space. Sci. Rev.* 174, 213–250. doi: 10.1007/s11214-012-9942-9.

Mumma M.J., Villanueva G.L., Novak R.E., Hewagama T., Bonev B.P., DiSanti M.A., Mandell A.M., and Smith M.D. 2009. Strong release of methane on Mars in northern summer 2003. *Science* 323:1041–1045.

Oze C., and Sharma M. 2005. Have olivine, will gas: Serpentinization and the abiogenic production of methane on Mars, *Geophys. Res. Lett.* 32, L10203.

Phillips R.J., Zuber M.T., Solomon S.C., Golombek M.P., Jakosky B.M., Banerdt,W.B., Williams R.M.E., Hynek B.E., Aharonson O., and Hauck II S.A. 2001. Ancient geodynamics and global-scale hydrology on Mars. *Science*, 291:2587-2591. doi: 10.1126/science.1058701

Popova O., Nemtchinov I., Hartmann W. K. 2003. Bolides in the present and past martian atmosphere and effects on cratering processes. *Meteorit. Planet. Sci.* 38 (6), 905–925, doi:10.1111/j.1945-5100.2003.tb00287.x

Quesnel Y., Sotin C., Langlais B., Costin S., Mandea M., Gottschalk M., and Dyment J. 2009. Serpentinization of the martian crust during Noachian. *Earth Planet. Sci. Let.* 277:184–193. doi: 10.1016/j.epsl.2008.10.012.

Ramirez R.M., Kopparapu R., Zugger M.E., Robinson T.D., Friedmann R., and Kasting J.F. 2014. Warming early Mars with CO_2 and H_2. *Nat. Geosci.*, 7, 59-63, doi: 10.1038/NGEO2000.

Robbins S. J., Hynek B. M., Lillis R. J., and Bottke W. F. 2013. Large impact crater histories of Mars: The effect of different model crater age techniques. *Icarus*, *225*(1), 173-184.

Roberts J.H., and Zhong, S. 2007. The cause for the north-south orientation of the crustal dichotomy and the equatorial location of Tharsis on Mars. *Icarus* 190. doi: 10.1016/j.icarus.2007.03.002.

Schmidt F., Chassefière, E., Tian, F., Dartois, E., Herry, J.-M., Mousis O. 2016. Early Mars volcanic sulfur storage in the upper cryosphere and formation of transient SO_2-rich atmospheres during the Hesperian, *Meteoritics & Planetary Sciences*, this issue, accepted for publication.

Segura T. L., Toon O. B., Colaprete A., and Zahnle K. (2002). Environmental effects of large impacts on Mars. *Science* 298(5600), 1977-1980.

Segura T.L., Toon O.B., Colaprete A. 2008. Modeling the environmental effects of moderate-sized impacts on Mars. *J. Geophys. Res.* 113, E11007. doi:10.1029/ 2008JE003147.

Segura T. L., McKay C. P., and Toon O. B. (2012). An impact-induced, stable, runaway climate on Mars. *Icarus* 220(1), 144-148.

Solomon S.C., Aharonson O, Aurnou J.M., Banerdt W.B., Carr M.H., Dombard A.J., Frey H.V., Golombek M.P., Hauck II S.A., Head III J.W., Jakosky B.M., Johnson C.L., McGovern P.J., Neumann G.A., Phillips R.J., Smith D.E., and Zuber, M.T. 2005. New Perspectives on Ancient Mars. *Science* 307, 1214, doi:10.1126/science.1101812.

Tian F., Kasting J.F., and Solomon S.C. 2009. Thermal escape of carbon from the early Martian atmosphere. *Geophys. Res. Lett.* 36, L02205, doi/10.1029/2008GL036513.

Tian F., Claire M.W., Haqq-Misra J.D., Smith, M., Crisp D.C., Catling D., Zahnle K., and Kasting J.F. 2010. Photochemical and climate consequences of sulfur outgassing on early Mars. *Earth Planet. Sci. Lett*. 295, 412-418.

Tsai V.C., and Stevenson D.J. 2007. Theoretical constraints on true polar wander. *J. Geophys. Res.*, 112, B5, doi:10.1029/2005JB003923.

Van Berk W., Fu Y., and Ilger J.-M. 2012. Reproducing early Martian carbon dioxide partial pressure by modeling the formation of Mg-Fe-Ca carbonate identified in the Comanche rock outcrops on Mars. *J. Geophys. Res.* 117, E10008, doi:10.1029/2012JE004173.

Villanueva G.L., Mumma M.J., Novak R.E., Radeva Y.L., Käufl H.U., Smette A., Tokunaga A., Khayat A., Encrenaz T., and Hartogh P. 2013. A sensitive search for organics (CH_4, CH_3OH, H_2CO, C_2H_6, C_2H_2, C_2H_4), hydroperoxyl (HO_2), nitrogen compounds (N_2O, NH_3,

HCN) and chlorine species (HCl, CH_3Cl) on Mars using ground-based high-resolution infrared spectroscopy. *Icarus*, doi: 10.1016/j.icarus.2012.11.013.

Webster C.R., Mahaffy P.R., Atreya S.K., Flesch G.J., Farley K.A., and MSL Science Team. 2013. Low Upper Limit to Methane Abundance on Mars. *Science* doi: 10.1126/science.1242902.

Webster C.R., Mahaffy P.R., Atreya S.K., Flesch G.J., Mischna M.A., Meslin P.Y., Farley K.A., Conrad P.G., Christensen L.E., Pavlov A.A., et al. 2014. Mars methane detection and variability at Gale crater. *Science* doi: 10.1126/science.1261713.

Welhan J.A., Craig H. 1979. Methane and hydrogen in East Pacific rise hydrothermal fluid. *Geophys. Res. Lett.* 6 (11), 829–831.

Werner S.C. 2009. The global martian volcanic evolutionary history. *Icarus* 201, 44-68.

Zahnle K., Haberle R.M., Catling D.C., and Kasting J.F. 2008. Photochemical instability of the ancient Mars atmosphere. *J. Geophys. Res*. 113, E11004.1-E11004.16.

Zanhle K., Freedman R.S., and Catling, D.C. 2011. Is there methane on Mars?, Icarus 212, 493-503.

Zahnle K. and Catling D.C. 2015. Play it again, SAM !, *Science* 347, 6220, 370-371, DOI: 10.1126/science.aaa3687.

Zhong, S. 2009. Migration of Tharsis volcanism on Mars caused by differential rotation of the lithosphere, *Nat. Geosc*., 2, doi: 10.1038/NGEO392.

FIGURE CAPTIONS

Figure 1: Existing observational, geochemical modelling and theoretical constraints on paleopressure of the Martian atmosphere (colored boxes and circles with arrows) and derived scenario of pressure evolution (thick black line). Observational and modelling constraints are represented by, respectively, green and black texts and box contours. The scenario consists in (i) an initially large pressure with a subsequent continuous decrease of the pressure due to hydrodynamic escape; (ii) then a stabilization of the pressure around 1.5 bar, compatible with both the upper limit of 2 bar, above which CO_2 condenses into clathrates at the Noachian (left blue box), and the lower limit of 1.3 bar, below which the addition of H_2 is not efficient in raising the surface temperature above the H_2O freezing point at the Hesperian (orange box); (iii) a drop of the pressure from 1.5 bar to below 0.5 bar, which could explain the formation of massive sulfate deposits at this epoch due to the decomposition of CO_2-SO_2 clathrates (right blue box), and is compatible with the constraint derived from crater analysis (green box). Adapted from Kite et al. (2014).

Figure 2 : Depth of a clathrate cryosphere as a function of the latitude with an exponential decay of porosity starting at 20% on the surface, and for 50 and 100 $mW.m^{-2}$ geothermal heat fluxes. (adapted from the Clifford et al., 2010 subsurface model). The maximum and minimum variations due to the obliquity and eccentricity variations of Mars orbit are shown (based on Laskar 2004 simulations).